Korean J. Chem. Eng., 35(2), 526-534 (2018)
DOI: 10.1007/s11814-017-0282-z

pISSN: 0256-1115
eISSN: 1975-7220

Aminosilane grafted Matrimid 5218/nano-silica mixed matrix membrane for CO_2/light gases separation

Elham Nezhadmoghadam*, Mahdi Pourafshari Chenar*, Mohammdreza Omidkhah, Amir Nezhadmoghadam*, and Reza Abedini***,†**

*Department of Chemical Engineering, Faculty of Engineering, Ferdowsi University of Mashhad, Mashhad, Iran
**Faculty of Chemical Engineering, Tarbiat Modares University, Tehran, Iran
***Faculty of Chemical Engineering, Babol Noshirvani University of Technology, Babol, Iran
(*Received 19 June 2017 • accepted 7 October 2017*)

Abstract−The influence of amino-grafted nano-silica particles on the CO_2/light gases separation performance of Matrimid mixed matrix membrane was evaluated. The aminosilane grafting reaction was performed using (3-aminopropyl) terimethoxysilane (APTMOS) as a silane coupling agent. Prepared membranes were studied through various methods including FTIR, SEM and TGA. To evaluate the gas separation performance, pure CO_2, CH_4, N_2 and O_2 permeation tests were conducted using constant volume-varying pressure set-up with various upstream pressures. Characterization results demonstrated the appropriate dispersion of silica particles within the Matrimid matrix as well as a suitable interaction between polymer/filler phases. Results from the gas permeation study confirmed that the permeability of all gases except CO_2, decreased as silica content increased in Matrimid matrix. Nevertheless, the CO_2 permeability increased from 4.20 Barrer in neat Matrimid to about 9.59 Barrer at 20 wt% loading of silica. The selectivity of O_2/N_2, CO_2/N_2 and CO_2/CH_4 pair gases was enhanced by increasing the nano-silica content. The selectivity of CO_2/N_2 and CO_2/CH_4 was increased from 18.27 to 50.74, and 20.01 to 70.51, respectively.

Keywords: Mixed Matrix Membrane, Matrimid, Nano-silica, Grafting, CO_2 Separation

INTRODUCTION

Polymeric membrane has gained more interest for use in gas separation industries (i.e., air separation, gas sweetening, CO_2 capturing, hydrogen recovery etc.) [1-3]. Ease of fabrication, lower cost, working at lower temperature and simple scalability are the major reasons for application of membrane in gas separation [3,4]. In spite of these advantages, the trade-off between gas permeability and selectivity leads to the restriction of membrane application, as reported by Robeson [5]. Consequently, the aim of recent studies was to propose a solution to overcome the Robeson bound, and finally using the inorganic particles in polymeric membrane was recommended [6,7]. In fact, mixed matrix membranes MMMs are comprised of two phases, a polymeric bulk phase and dispersed inorganic particles such as carbon molecular sieves, nano-sized metal oxide or zeolites. MMMs also combine the advantages of polymers and inorganic additives, including process ability of polymers and high selectivity as well as proper mechanical properties [7].

Ahn et al. evaluated the performance of MMM comprised of nano-sized silica particles and glassy polysulfone on gas permeation properties of resultant membranes. Their findings revealed that adding the silica particles enhanced the gas separation properties of polysulfone significantly. The permeability enhancement was assigned to the increase of membrane free volume due to incorporated particles [8].

A mixed matrix membrane comprising polyimide and silica nano-particles to separate CO_2 and CH_4 was evaluated by Suzuki et al., whose study stated that the CO_2 permeability in MMMs increased as the silica loading increased. Despite that, CO_2 behavior, CH_4 permeability coefficient decreased with increasing silica weight percent because of lower value of CH_4 diffusivity. Accordingly, CO_2/CH_4 selectivity of MMMs improved surprisingly [9].

Sadeghi et al. investigated the ability of EVA/silica MMM for CO_2/N_2 and CO_2/CH_4 pair gases separation. Their obtained results demonstrated that the gases' permeability increased by increasing the silica content in polymer matrix. Moreover, CO_2/N_2 and CO_2/CH_4 selectivities were enhanced significantly [10].

Hassanajili et al. examined the effect of hydrophobic SiO_2 and Polyesterurethane MMMs for gas separation. The silica nanoparticles were modified with octylsilane and PDMS. The hydrophobic chains contain fillers that reduce the aggregation of nanoparticles, and improve the dispersion more than unmodified particles in MMMs. The unmodified silica nanoparticles expose better CO_2 permeability and CO_2/CH_4 selectivity than other fillers [11].

Ghadimi et al. fabricated the MMMs comprised of SiO_2 and poly (ether block amide) (PEBA) by means of different approaches, including sol-gel, and surface modification by physical and chemical methods. Poly (ethylene glycol) (PEG) and cis-9-octadecenoic acid (OA) were used as surface modification precursors on silica spheres by chemical modification. The surface modified SiO_2 nanoparticles thereby enhanced their distribution in the PEBA matrix, and the best gas separation was obtained with OA-SiO_2 due to the

†To whom correspondence should be addressed.
E-mail: abedini@nit.ac.ir

removal of the filler agglomeration matrix [12].

Based on the investigated studies, the incorporated nano-silica particles in polymer led to the gas transport enhancement. Note that the physicochemical character of based polymer has evident role in gas transport behavior. The glassy and rubbery nature of polymer matrix caused the prepared membrane to show different gas permeation property [13]. Glassy polymers introduce high selective membrane based on a sieving character as well as proper mechanical properties. Using the rubbery polymers to fabricate membrane exhibits a higher gas permeation and the selectivity of resultant membrane controlled by the degree of gases condensability [14]. Polyimides are the main type of glassy polymers used widely to separate/capture of CO_2 from gas streams. Matrimid is an outstanding aromatic polyimide and is employed as a based polymer to separate CO_2 selectively. Additionally, Matrimid®5218 compared to other commercial polymers such as cellulose acetate, polysulfone, and polyethersulfone shows a superior CO_2/light gases selectivity [15].

In this work, we used nano-silica particles as inorganic fillers and incorporated into Matrimid®5218 to form MMMs with improved CO_2 separation. Silica particles were synthesized through sol-gel method and added to the casting solution with different weight percent (0 to 20 wt%). Prepared membranes where characterized by means of SEM, FTIR and TGA methods. Furthermore, a constant volume-varying pressure gas permeation set-up was used to examine the separation performance of as prepared MMMs.

The gas transport properties of prepared MMMs studied using and the CO_2, CH_4, N_2 and O_2 permeabilities were calculated.

MATERIALS AND METHODS

1. Materials

Matrimid 5218 used as a polymer phase for membranes was purchased from Huntsman LLC. N-methyl-2-pyrolidone (NMP) with the purity of 99.99% was supplied by Merck Co. Tetraethylorthosilicate (TEOS), 3-aminopropyl terimethoxysilane (APTMOS), ethanol and hydrochloric acid were purchased from Merck Co.

2. Sol-gel Synthesis of Matrimid/Silica Nano-composite Membrane

Silica nano-particles were synthesized using the TEOS hydrolysis in ethanol and presence of HCl as a catalyst. First, 25 g of TEOS with 4 g of APTMOS as a coupling agent was mixed in 30 mL of ethanol at the temperature of 75 °C for 1 h. After that, a mixture of ethanol (30 mL), de-ionized water (7.5 g) and HCl (0.83 g) was added to the mixture dropwise. The stirring of mixture was continued for 1 hr to form a clear silica-sol. The desired value of silica-sol was added to the NMP and mixed for 2 hr. Then, Matrimid was dissolved in NMP for 24 hr. To remove the bubbles created during the stirring process, the created solution was degassed in an ultrasonic bath and the obtained homogeneous solution was cast on a flat glassy plate with film applicator. The cast solution was dried in a vacuumed oven at 120 °C for 24 h. Finally, the created membrane was easily separated from the glass plate.

3. Membrane Characterization

Fourier transform infrared spectrometer (FT-IR; PerkinElmer-10.03.06) was used to study the created changes in chemical structure of membranes due to cross-linking. For each specimen, 32 scans were collected with a wavenumber resolution of 4 cm^{-1}.

Scanning electron microscopy (SEM) was employed to study the cross sectional morphology of membranes as well as the quality of silica dispersion. All MMMs were snapped in liquid nitrogen for unfailed and clean cut. The membrane surfaces were coated with gold metal using the BAL-TEC SCD 005 sputter coater (BAL-TEC AG, Balzers, Liechtenstein). Finally, the SEM images of prepared samples were taken using a CamScan SEM model MV2300 microscope.

To investigate the degradation temperature and thermal stability of membranes, thermal gravimetric analyzer (TGA-50, Shimadzu) was used. For all study, 15 mg of sample was loaded in a pretarred platinum pan and pre-heated above 120 °C to remove any moisture. After cooling, the sample was reheated from 20 to 800 °C with a rate of 10 °C/min.

4. Permeation Study

The gas separation property of each membrane was assessed by measuring the CO_2, CH_4, N_2 and O_2 gas permeability in a constant volume/variable pressure system. The membrane was placed in a permeation cell comprised of two separate parts and was sealed with O-rings. For accurate gas permeability measurement, the set-up was evacuated and residual air or other possible gases were removed. The feed gas was introduced to the cell from the upstream, whereas the downstream was under high vacuum. The pressures on both sides were monitored online using pressure transducers.

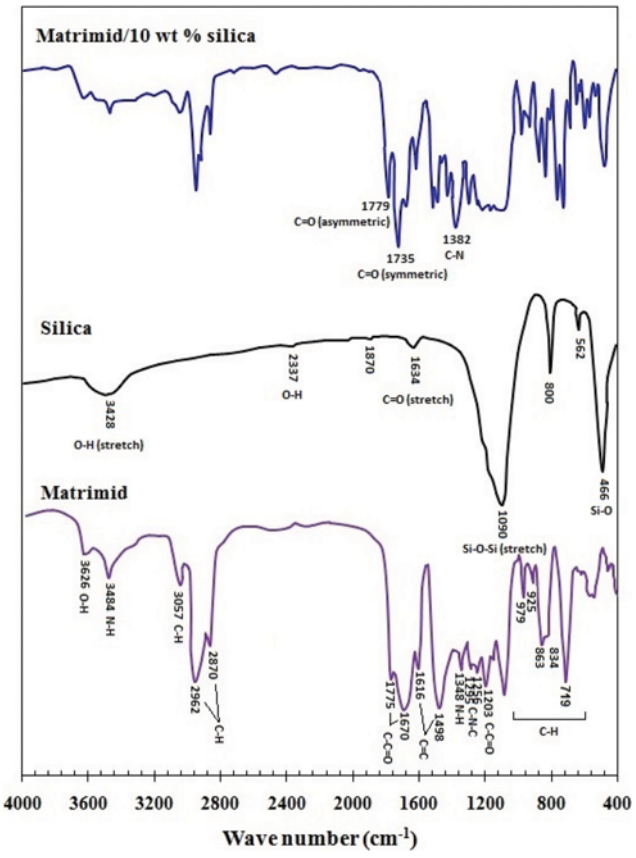

Fig. 1. FTIR spectra of neat Matrimid, silica particles and Matrimid/10 wt% silica MMM.

A permeate gas from the membrane was collected in a constant volume downstream, and the correspondent pressure rise was measured online by an absolute pressure transmitter (type 691, Huba Control, Wurenlos, Switzerland).

The permeability (P) in Barrer (1 Barrer=1×10^{-10} cm^3(STP)-cm/cm^2·s·cmHg), was calculated by using the steady-state rate of pressure increase (dp/dt, mmHg/s) in a constant permeate volume with the following equation (Eq. (1)):

$$P = \frac{273.15\times10^{10}Vl}{760AT\left(\frac{P_o\times76}{14.7}\right)}\frac{dp}{dt} \quad (1)$$

where V is the volume of vessel (cm^3), T is the operating temperature (K), l is the membrane thickness (cm), A is the effective membrane area (cm^2) and P_o is feed pressure in psia. Permeability measurements were performed at a feed pressure in a range of 2-10 bar. The ideal selectivity of two pure gases was calculated by dividing the accordance permeability values as shown in Eq. (2).

$$\alpha = \frac{P_{CO_2}}{P_{CH_4}} \quad (2)$$

To calculate the diffusivity coefficient of each gas in membrane, the time lag method for MMMs was used (Eq. (3)).

$$D = \frac{L^2}{6\theta} \quad (3)$$

where L is the membrane thickness (cm) and θ is the time lag (s).

A multiplication of diffusivity and solubility can gives the permeability of gases in membranes.

Thus, gas solubility in membrane matrix can be determined as follows:

$$S = \frac{P}{D} \quad (4)$$

RESULTS AND DISCUSSION

1. Characterization

The FTIR spectra of neat Matrimid, silica nano-particles and Matrimid/10 wt% of silica are depicted in Fig. 1. For neat Matrimid, a characteristic band at 1,775 cm^{-1} corresponds to C=O stretching bond owing to the ketonic group (asymmetric stretch

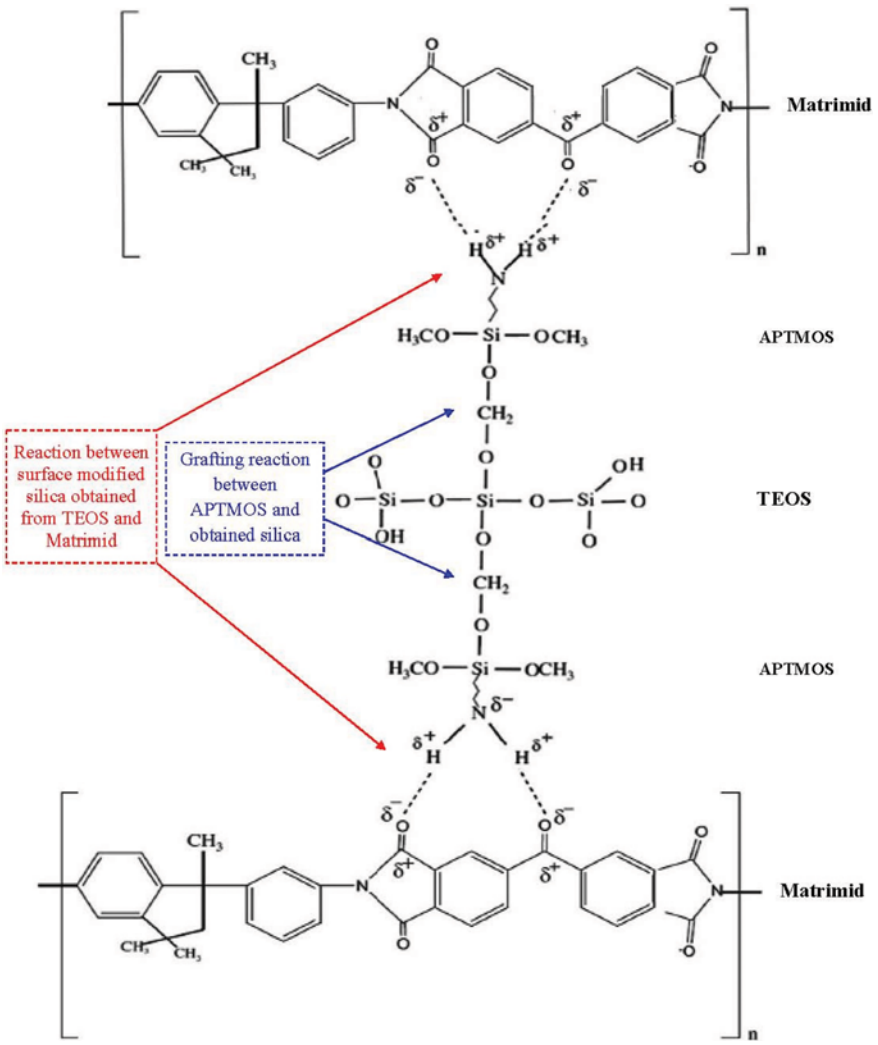

Fig. 2. The interaction of each functional group including APTMOS and obtained silica and Matrimid/silica.

vibration of 5-membered imide ring carbonyl) and furthermore a peak at 1,670 cm^{-1} ascribed to imidic group (symmetric stretch vibration of benzophenone carbonyl) [16]. The aromatic double bonds (C=C) stretching vibrations are introduced by the peaks at 1,498 and 1,616 cm^{-1}. The adsorption bands at 2,870 and 2,962 cm^{-1} are attributed to the C-H stretching of aliphatic rings, while the aromatic one attends at 3,057 cm^{-1} [17]. In addition, the peaks of C-H stretching due to the CH_2 deformation are observed at 700-1,000 cm^{-1}. The Matrimid spectrum exhibits the characteristic bands at 1,256, 1,295 cm^{-1} due to the bending/stretching vibrations of C-N-C bond in the imide ring. The bands at 1,348 and 3,484 cm^{-1}, correspond to the N-H bonds of secondary bending/stretching amine vibrations, respectively [18].

Fig. 1 also depicts the FTIR spectra of silica particles. The bands between 3,500-3,000 cm^{-1} correspond to the -OH stretching. The band at 1,634 cm^{-1} is related to the C=O stretching [19]. 1,629 and 1,381 cm^{-1} correspond to the H-O-H bending and C-H deformation. Asymmetric Si-O-Si stretching is defined at 1,090 cm^{-1}. Si-OH stretching and symmetric Si-O-Si stretching are obvious at 592 and 800 cm^{-1} [20].

Fig. 2 illustrates the spectra of Matrimid/10 wt% silica. It is evident that all corresponding imide bands are preserved. In general, the peak intensity of Matrimid was decreased by incorporating the silylated particles. The bands at 3,484 cm^{-1} and 2,700 to 3,100 cm^{-1} which correspond to the N-H and C-H bonds, respectively, are harshly weakened induced by the overlapping the O-H stretching band of silica particles (3,000-3,600 cm^{-1}) [21,22]. Moreover, the C=O stretching bands attributed to ketonic and imidic group (1,775 and 1,670 cm^{-1}) are shifted to the sharper peaks. Actually, the amino group of APTMOS reacts with imide group of Matrimid and leads to the formation of covalent bond between these phases. Furthermore, the strong interaction between Matrimid and aminosilane coupling agent is shown in Fig. 2 schematically. The formatted hydrogen bond between Matrimid (C=O group) and silica (OH group) also leads to the prevention of non-selective void at the Matrimid/silica interface that resulted in selectivity enhancement.

The membrane morphology has a strong effect on gas trans-

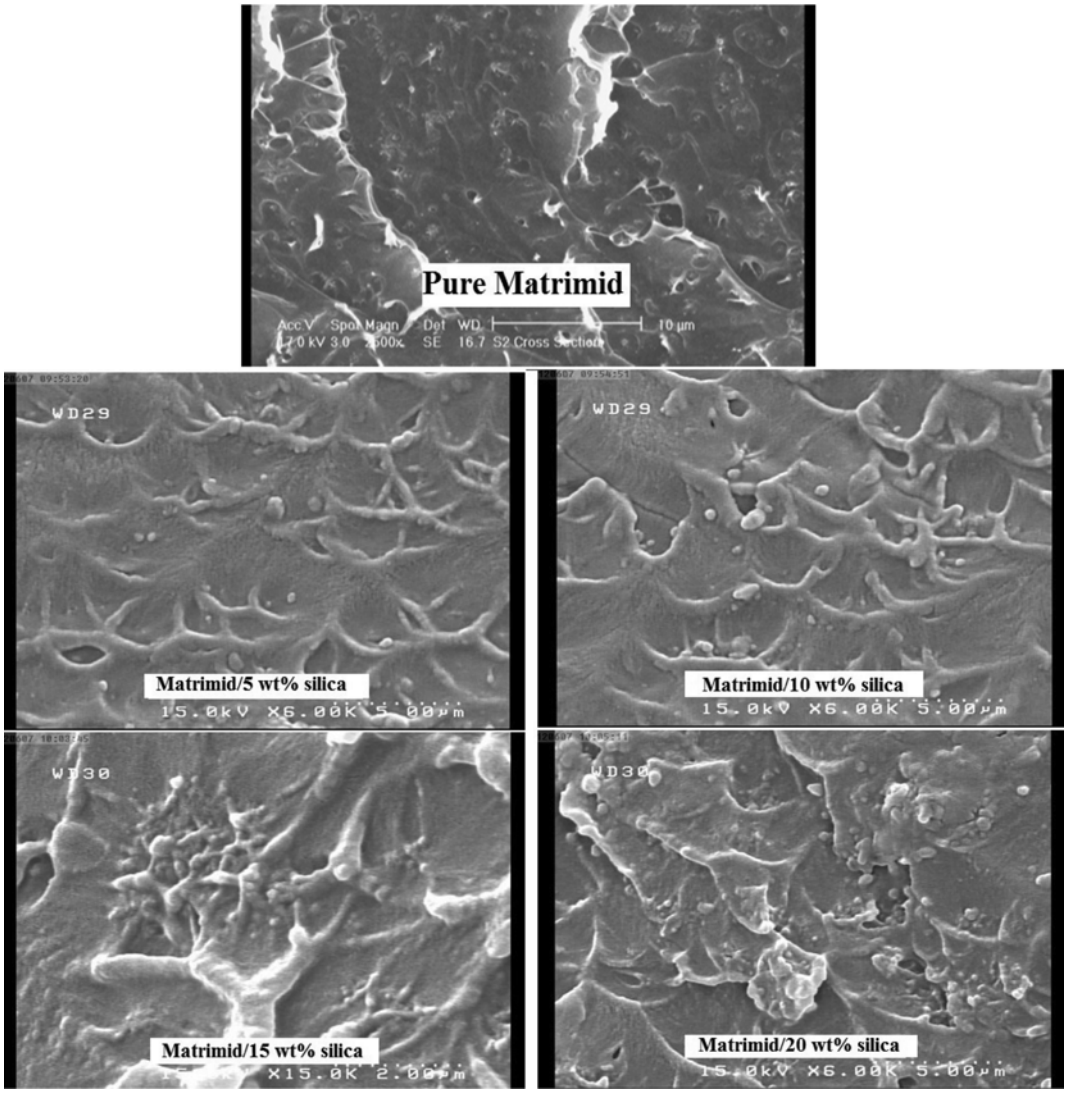

Fig. 3. Cross sectional morphology of each MMMs obtained by SEM.

port properties of MMMs. The morphology studies of Matrimid/silica MMMs were carried out by means of SEM analysis. Fig. 3 demonstrates the SEM cross sectional image of neat Matrimid and MMMs. It can be seen that at lower content of fillers, the more uniform dispersion of particles was achieved. The proper distribution of silica particles within the polymer matrix indicates that fine polymer/filler compatibility was established that can be related to the created hydrogen bonding between silica and Matrimid. Moreover, the compatibility of silica particles and polymer chains due to the presence of APTMOS is good. As silica content increases in Matrimid matrix, the smooth and integrated pattern of Matrimid is missing. The created grooved pattern due to the presence of nano-particles shows the appropriate compatibility of polymer phase and additive [23], as it is shown in Fig. 3. The grooved-pattern was intensified in cross section of nano-composite membranes as silica content increased. The existing stress in interface of polymer and particles leads to creation of unremitting debonding of Matrimid/silica MMMs.

Generally, increasing the inorganic filler concentration in polymer matrix increases the possibility of particle agglomeration. In this case, at higher loading of silica content (i.e., 15 and 20 wt%) the intensity of agglomeration phenomenon increased because of the lack of interaction with the polymer matrix. This can lead to void creation at the interface of agglomerated silica and polymer matrix.

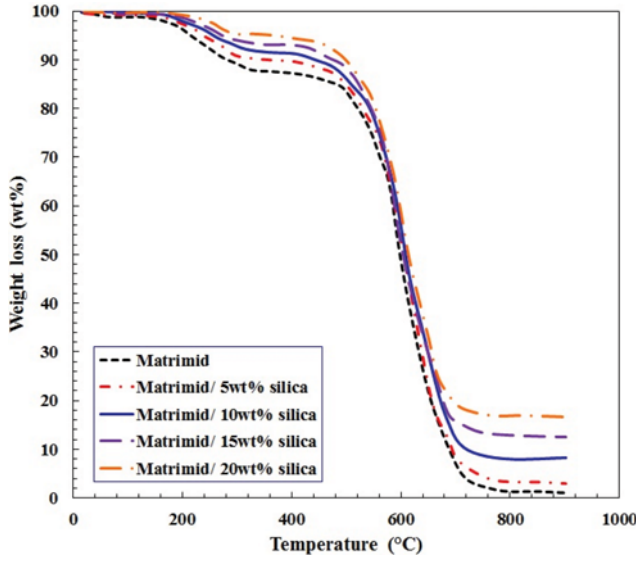

Fig. 4. TGA curves of Matrimid and MMMs containing silica (5-20 wt%).

Thermal stability of neat Matrimid and Matrimid/silica MMMs was evaluated by means of TGA method, and the corresponding results are shown in Fig. 4. As shown, the TGA curves for each membrane show three intrinsic steps: the first step at about 200-300 °C, the second at 480-750 °C, and the third is located at 750 °C to the higher temperature. These steps are attributed to the solvent evaporation within the membrane matrix, thermal degradation of polymers and carbonization of polymer chains, respectively. The polymer degradation of neat Matrimid started from 220 °C and continued to about 750 °C. For MMMs containing silica particles, the degradation temperature started at elevated temperature owing to the strong interaction between Matrimid and silica induced by hydrogen bonding, which imprisons the thermal motion of polymer and through this, the amount of energy required for polymer chains movement or segmentation increases [24]. Thereby, the thermal stability of MMMs would be enhanced compared to neat Matrimid.

2. Gas Permeation Study

Table 1 lists the amount of gas permeability of neat Matrimid and MMMs at different silica content. According to the obtained results, the CO_2 permeability is considerably higher than other gases in each membrane. The superior permeability of CO_2 compared to O_2, N_2 and CH_4 is assigned to its lower kinetic diameter, more condensability, and also the interaction that can be created between the polar CO_2 and polar groups of Matrimid [25,26].

Results showed that Matrimid membranes transport gases based on their kinetic size, and gas permeability is shown the below order:

$$P_{CO2}>P_{O2}>P_{N2}>P_{CH4}$$

Thus, the diffusion mechanism seems to be dominant in gas permeation through the glassy Matrimid. Therefore, the obtained results show the high glassy properties of neat and MMMs. Table 1 also reveals the effect of silica incorporation to Matrimid matrix on the gas permeability. Results show that embedding silica particles to Matrimid tends to decrease the permeability of O_2, N_2 and CH_4 gases, while the permeability of CO_2 increases. CO_2 permeability improves from 4.20 Barrer at no silica loading to 9.59 Barrer at 20 wt% of silica. Generally, when impermeable particles such as silica are added to the polymer matrices, the permeability of gases decreases [27].

The membrane gas permeation properties can be described by solution-diffusion mechanism that relates solubility and diffusivity of penetrant in polymer matrix. To interpret the gas permeability through a membrane, the gas diffusivity and solubility were calcu-

Table 1. Permeability and ideal selectivity of Matrimid and Matrimid/silica MMMs at 35 °C and 2 bar

Membrane Mat./silica (wt%)	Permeability (Barrer)				Selectivity		
	N_2	O_2	CH_4	CO_2	O_2/N_2	CO_2/N_2	CO_2/CH_4
100/0	0.23±0.1	1.28±0.2	0.21±0.3	4.20±1.6	5.56±0.4	18.27±3.0	20.01±0.5
95/5	0.22±0.1	1.27±0.2	0.19±0.3	4.90±1.7	5.61±0.4	21.68±3.5	24.62±0.6
90/10	0.21±0.1	1.24±0.2	0.16±0.3	5.82±1.7	5.90±0.4	27.71±4.4	34.85±0.6
85/15	0.20±0.1	1.22±0.2	0.15±0.2	7.63±1.9	5.94±0.5	37.17±5.8	50.46±0.6
80/20	0.18±0.1	1.15±0.1	0.13±0.2	9.59±1.9	6.08±0.6	50.74±6.9	70.51±0.7

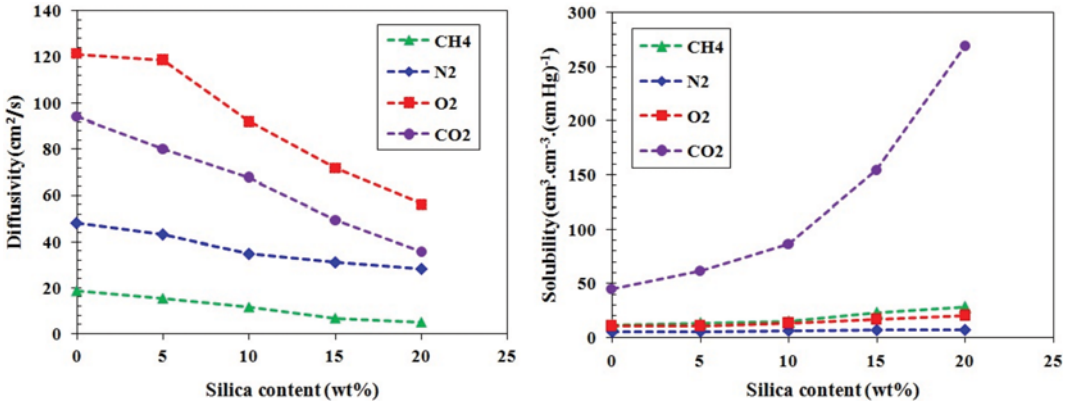

Fig. 5. Diffusivity and solubility coefficient of the gases in Matrimid and Matrimid/silica MMMs at 35 °C and 2 bar.

lated by applying time-lag method.

Fig. 5 depicts the diffusivity and solubility values of each gas in neat Matrimid and Matrimid/silica MMMs in terms of weight percent of silica particles. The obtained results demonstrate that increase of silica loading in the MMMs matrix leads to the reduction of the gas diffusivity. Generally, embedded silica caused the restriction of gas molecules transport in Matrimid by elongation of gas pathways through tortuosity and finally the gases diffusivity decreased [28].

Fig. 5 illustrates that variation of solubility coefficient of gases as silica content increases in Matrimid matrix, and results show the solubility enhancement, especially for more condensable gases. A potential surface of silica particles can assist the gas sorption and indicates that the reduction in CH_4, N_2 and O_2 permeability was ascribed to the diffusivity reduction.

The enhancement in permeability of condensable CO_2 can be related to the increase in the number of sites for CO_2 dissolution in polymer matrix. Thus, the increment in CO_2 permeability at higher silica loading is attributed to the CO_2 solubility improvement, while its diffusivity reduced. The comparison between gases' solubility shows that CO_2 solubility increases up to 26.93, but other gases have much lower increment.

Indeed, the embedded silica in Matrimid matrix increases the polar OH sites and intensifies the affinity of condensable CO_2 gas to absorb on polymer chains. Generally, the larger penetrants are more restricted to pass through the membrane as the polymer free volume is reduced. Accordingly, the significant methane permeability reduction compared to O_2 and N_2 is assigned to its larger molecular size.

The parameter $(P_{MMM}-P_P)/P_P$ can be defined as silica contribution to permeability of each gas, where P_{MMM} and P_P are the permeability of MMM and neat Matrimid, respectively. Hence, the influence of silica on each gas permeability in MMMs compared to neat membrane can be evaluated. Counting on the value of P_{MMM}, this parameter can be negative, zero or positive. The negative value implies the stalled permeation, zero value means that silica particles has no net effect on gas permeability, and finally the positive ones cause the facilitation effect of silica. Fig. 6 represents the contribution of silica particles at different loading to gases permeability. The contribution of silica to permeability of larger condensable CO_2 was evident and thus, the presence of silica in polymer matrix facilitates permeation of the larger CO_2. The reduction values of gases permeability of MMMs containing 20 wt% silica compared to neat Matrimid shows the following order:

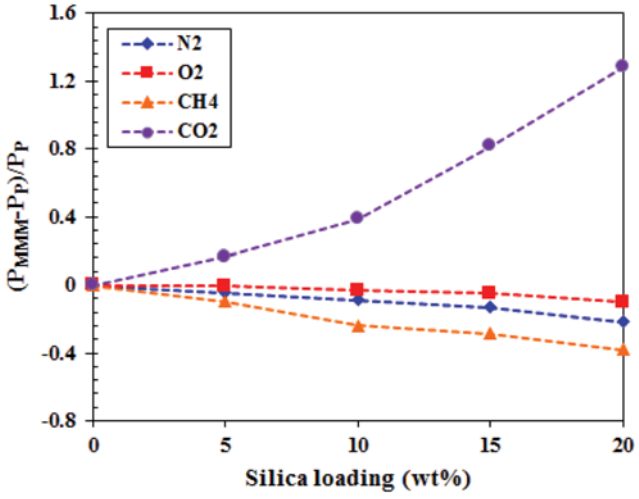

Fig. 6. The contribution of silica to gases permeability at each particle loading.

CH_4 (38.0%)>N_2 (21.7%)>O_2 (10.1%)

Table 1 also lists the O_2/N_2, CO_2/N_2 and CO_2/CH_4 selectivity of Matrimid and Matrimid/silica MMMs. Results indicate that increase in silica loading tends to the selectivity improvement of each gas pair. A comparison between pair selectivities demonstrates that O_2/N_2, CO_2/N_2 and CO_2/CH_4 selectivities increase up to 9, 177 and 252%.

As mentioned earlier, N_2, O_2 and CH_4 permeability was reduced as silica content increased, whereas CO_2 permeability increased upon the high interaction between condensable CO_2 and polar OH groups. Thus, selectivities, those including CO_2 are quite high, especially in the case of CO_2/CH_4. As methane gas has a larger molecular size, it is more restricted to cross the polymer matrix, and thereby CO_2/CH_4 selectivity increases more than one CO_2/N_2. Moreover, the sieving character of filled membranes is enhanced

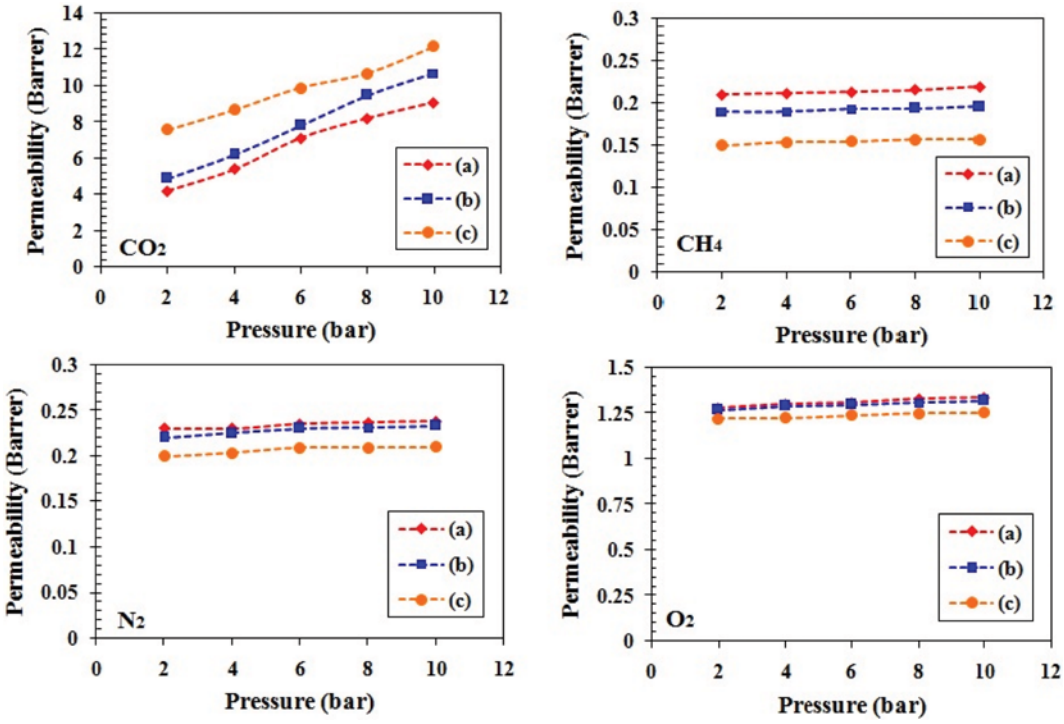

Fig. 7. Effect of feed pressure on gases permeability for (a) neat Matrimid and MMMs those containing (b) 5 and (c) 15 wt% of silica.

as the silica content increases, which offers an improvement in O_2/N_2 pair gases' selectivity owing to their non-condensable property.

Fig. 7 illustrates each gases' permeability in neat Matrimid and Matrimid filled with 5 and 15 wt% of silica particles versus feed pressure. In fact, the mechanism of gas permeation can be explained by scrutinizing the permeability variation versus trans-membrane pressure.

As Fig. 7 presents, the permeability of all gases except CO_2 in Matrimid and Matrimid/silica MMMs remains almost constant or increases slightly in terms of pressure increment. Conversely, the CO_2 permeability increases as pressure increases. The improvement in CO_2 permeability in terms of feed pressure can be assigned to the greater sorption of condensable CO_2. Moreover, higher interaction between polar CO_2 and OH group at elevated pressure can be expected [29]. Besides, increasing the pressure has two main effects on polymer matrix which can control the gases' permeability. At higher feed pressure, the CO_2 concentration increases, and thereby the polymer plasticization is intensified. Conversely, introducing gases to membrane at elevated pressure causes the polymer chains compactness and reduction of fractional free volume, which

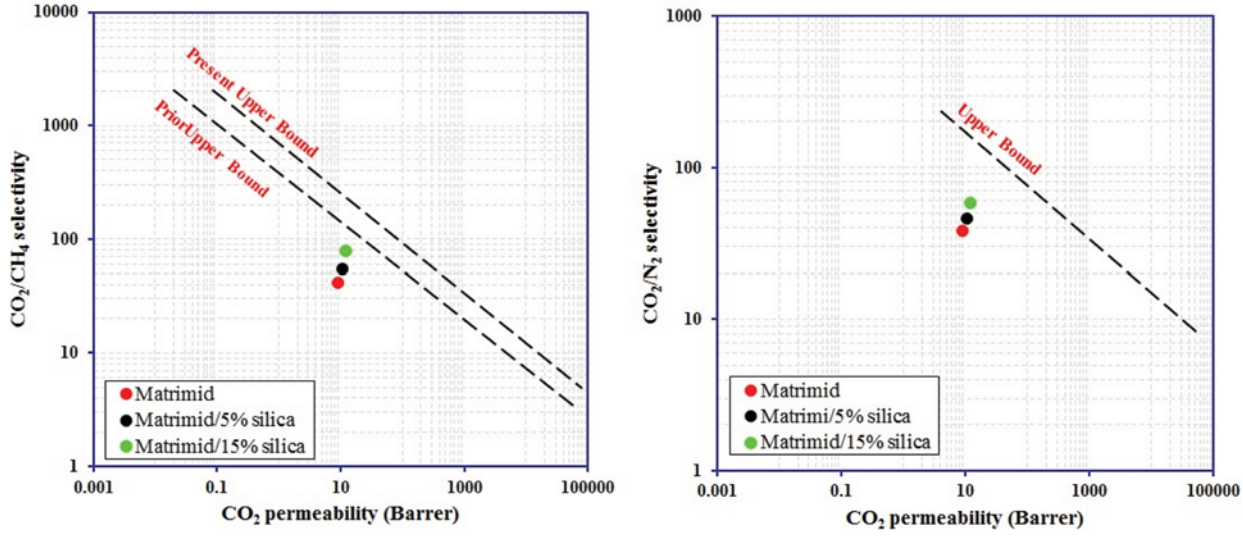

Fig. 8. Membranes performance in CO_2/CH_4 and CO_2/N_2 separation at pressure of 10 bar compared to Robeson bound.

Table 2. A comparison between CO_2/CH_4 and CO_2/N_2 separation data for selected silica based MMMs and this work

Polymer	Filler	Loading (wt%)	Conditions		P_{CO_2}	$\frac{P_{CO_2}}{P_{CH_4}}$	$\frac{P_{CO_2}}{P_{N_2}}$	Ref.
			P	T				
6FDA	Silica (TAPOB)	10	2 bar	25 °C	7.4	74.2	33.6	9
EVA	Silica (TEOS)	10	8 bar	25 °C	47.3	0.38	27.5	10
Polyurethane	Silica (OS)[a]	15	10 bar	35 °C	6.96	9.9	28.4	11
Pebax	Silica (TEOS)	30	2 bar	25 °C	41.8	16.0	64.3	12
PVA	Silica (TEOS)	20	5 bar	35 °C	0.2	27.2	18.1	19
Matrimid5218	Silica (TEOS)[b]	15	10 bar	35 °C	12.1	77.5	57.6	This work

[a]Silica modified by octylsilane
[b]Silica grafted by aminosilane

results in gases' diffusion being diminished [30]. Finally, the net effect of these interactions results in the CO_2 permeability enhancement.

Fig. 8 represents the performance of MMMs in CO_2/CH_4 and CO_2/N_2 separation at the pressure of 10 bar compared to Robeson upper bound. As can be seen in Fig. 8, increasing the nano-silica content results in the closing to the Robeson bound. Consequently, the prepared MMMs have great potential to be applied in gas separation processes to separate CO_2 from light gases which prevents the spreading of the greenhouse CO_2 in the atmosphere.

Table 2 summarizes the results of CO_2/CO_4 separation using MMM in which silica particles were used as a filler. As is shown, the permeability and selectivity of each MMM are strong functions of polymer matrix and the nature of silica particles. Comparison of the results of this study with those of previously published work shows that aminosilane grafted Matrimid/silica MMMs have significantly higher selectivity.

CONCLUSIONS

MMMs comprised of Matrimid and nano-silica particles (0-20 wt%) were prepared to separate CO_2 from light gases. Obtained results from characterization methods revealed that the proper interaction between polymer and filler was achieved. Moreover, the thermal stability of MMMs was enhanced as the silica content increased within the polymer matrix. SEM images demonstrated that good particle dispersion occurred except at higher loading of filler where some particle agglomeration was seen. The gas permeation results revealed that the CO_2 permeability increased and also the CO_2/N_2 and CO_2/CH_4 selectivities were improved. The best-yield Matrimid/20 wt% MMM showed superior CO_2 and CO_2/CH_4 selectivity of 9.49 Barrer and 70.51, respectively. Increasing the feed pressure up to 10 bar, resulted in permeability rising of CO_2 where no obvious change was seen for CH_4, O_2 and N_2 permeabilities. Finally, the comparison between MMMs performance and the Robeson bound indicated that the embedded nano-silica improved the MMM's ability to separate CO_2 from other gases significantly.

ACKNOWLEDGEMENT

Special thanks of the authors go to the Research Center for Membrane Processes of Tarbiat Modares University for providing the membrane fabrication equipment and gas separation pilot.

REFERENCES

1. F. Dorosti, M. Omidkhah and R. Abedini, *J. Nat. Gas. Sci. Eng.*, **25**, 88 (2015).
2. M. Naghsh, M. Sadeghi, A. Moheb, M. Pourafshari Chenar and M. Mohagheghian, *J. Membr. Sci.*, **423**, 97 (2012).
3. Y. Zhang, J. Sunarsoc, S. Liud and R. Wang, *Int. J. Greenhouse Gas Cont.*, **12**, 84 (2013).
4. R. Abedini, M. Omidkhah and F. Dorosti, *RSC Adv.*, **4**, 36522 (2014).
5. M. Jamshidi, V. Pirouzfar, R. Abedini and M. Zamani Pedram, *Korean J. Chem. Eng.*, **34**, 829 (2017).
6. M. Sadeghi, M. A. Semsarzadeh, M. Barikani and M. Pourafshari Chenar, *J. Membr. Sci.*, **376**, 188 (2011).
7. R. Abedini, S. M. Mousavi and R. Aminzadeh, *Desalination*, **277**, 40 (2011).
8. J. Ahn, W. J. Chung, I. Pinnau and M. D. Guiver, *J. Membr. Sci.*, **314**, 123 (2008).
9. T. Suzuki and Y. Yamada, *Polym. Bull.*, **53**, 139 (2005).
10. M. Sadeghi, G. Khanbabaei, A. H. Saeedi Dehghani, M. A. Aravand, M. Akbarzade and S. Khatti, *J. Membr. Sci.*, **322**, 423 (2008).
11. S. Hassanajili, M. Khademi and P. Keshavarz, *J. Membr. Sci.*, **453**, 369 (2014).
12. A. Ghadimi, T. Mohammadi and N. Kasiri, *Ind. Eng. Chem. Res.*, **53**, 17476 (2014).
13. P. Bernardo, E. Drioli and G. Golemme, *Ind. Eng. Chem. Res.*, **48**, 4638 (2009).
14. H. Hosseinzadeh Beiragh, M. Omidkhah, R. Abedini, T. Khosravi and S. Pakseresht, *Asia-Pac. J. Chem. Eng.*, **11**, 522 (2016).
15. A. Ebadi Amooghin, M. Omidkhah and A. Kargari, *RSC Adv.*, **5**, 8552 (2015).
16. F. Moghadam, M. R. Omidkhah, E. Vasheghani Farahani, M. Z. Pedram and F. Dorosti, *Sep. Purif. Technol.*, **77**, 128 (2011).
17. F. Dorosti, M. Omidkhah and R. Abedini, Chem. *Eng. Res. Des.*, **92**, 2439 (2014).
18. M. Inagaki, N. Ohta and Y. Hishiyama, *Carbon.*, **61**, 1 (2013).
19. M. Mohagheghian, M. Sadeghi, M. Pourafshari Chenar and M. Naghsh, *Korean J. Chem. Eng.*, **31**, 2041 (2014).
20. S. Japip, H. Wang, Y. Xiao and T. S. Chung, *J. Membr. Sci.*, **467**, 162

(2014).
21. M. Waqas Anjum, F. de Clippel, J. Didden, A. L. Khan, S. Couck, G. V. Baron, J. F. M. Denayer, B. F. Sels and I. F. J. Vankelecom, *J. Membr. Sci.*, **495**, 121 (2015).
22. T. W. Pechar, M. Tsapatsis, E. Marand and R. Davis, *Desalination*, **146**, 3 (2002).
23. M. D. Guiver, G. P. Robertson, Y. Dai, F. Bilodeau, Y. S. Kang, K. J. Lee, J. Y. Jho and J. Won, *J. Polym. Sci. Part A: Polym. Chem.*, **40**, 4193 (2002).
24. R. Abedini, S. M. Mousavi and R. Aminzadeh, *Chem. Ind. Chem. Eng. Q.*, **18**, 385 (2012).
25. M. Sadeghi, M. M. Talakesh, B. Ghalei and M. Shafiei, *J. Membr. Sci.*, **427**, 21 (2013).
26. M. A. Semsarzadeh and B. Ghalei, *J. Membr. Sci.*, **432**, 115 (2013).
27. M. Sadeghi, M. A. Semsarzadeh and H. Moadel, *J. Membr. Sci.*, **331**, 21 (2009).
28. M. H. Nematollahi, A. H. Saeedi Dehaghani and R. Abedini, *Korean J. Chem. Eng.*, **33**, 657 (2016).
29. L. Wu, J. Sun and Y. Chen, *Mater. Des.*, **92**, 610 (2016).
30. R. Abedini, M. Omidkhah and F. Dorosti, *Int. J. Hydrogen Energy*, **39**, 7897 (2014).